# Thermal Stability Boundary of FG Panel under Aerodynamic Load

Sang-Lae Lee, and Ji-Hwan Kim

*Abstract*—In this study, it is investigated the stability boundary of Functionally Graded (FG) panel under the heats and supersonic airflows. Material properties are assumed to be temperature dependent, and a simple power law distribution is taken. First-order shear deformation theory (FSDT) of plate is applied to model the panel, and the von-Karman strain- displacement relations are adopted to consider the geometric nonlinearity due to large deformation. Further, the first-order piston theory is used to model the supersonic aerodynamic load acting on a panel and Rayleigh damping coefficient is used to present the structural damping. In order to find a critical value of the speed, linear flutter analysis of FG panels is performed. Numerical results are compared with the previous works, and present results for the temperature dependent material are discussed in detail for stability boundary of the panel with various volume fractions, and aerodynamic pressures.

*Keywords*—Functionally graded panels, Linear flutter analysis, Supersonic airflows, Temperature dependent material property.

## I. INTRODUCTION

METALS have been used in aerospace field as skin of supersonic flight vehicles for many years because of their excellent strength and toughness. However, the strength of a metal is reduced after it has been in a high-temperature environment for a period of time. To resist the high temperature, the surfaces of the metals are usually coated with a heat-proof material directly. For instance, the Space Shuttle utilizes ceramic tiles as thermal protection from heat generated during re-entry. However, since these tiles are laminated to the vehicle's superstructure they are prone to matrix cracking due to differences in thermal expansion coefficients between the tiles and the superstructure. Also, ceramic materials have excellent characteristics in strength and heat-resistance; nevertheless, their applications are usually limited due to their low toughness. To overcome these drawbacks of the composite materials, FGMs have been developed [1, 2].

In FGMs, made of ceramic and metal, the ceramic has a role to withstand significant heat conduction while the metal keeps a certain extent of toughness in a high-temperature environment. The mixture of the materials varies continuously from one interface to the other using gradual variation of the volume fraction for constituent materials. The FGM can be used for a skin panel of the spacecraft which suffers high temperature and high aerodynamic pressure during its launching and reentry status. When the vehicle flies at a supersonic speed, its skin panels may experience dynamic unstable state with self-excited oscillation. This phenomenon which is called as panel flutter can cause serious problems such as fatigue failure of the structure. This self-excited oscillation of external skin causes high amplitude lateral vibration of the skin panel with in-plane cyclic stresses and finally leads to the failure of the structure. Panel flutter is coalescence or merging frequency phenomena which is two of natural frequencies coalesce and become complex conjugate pairs.

Supersonic flutter characteristics of FG panels were studied by Prakash and Ganapathi[3] using FEM. They considered linear strains and showed that the use of FGM increases the flutter margin in comparison with metals. Praveen and Reddy [4] analyzed the nonlinear static and dynamic response of FG ceramic–metal plates in a steady temperature field using finite element method (FEM) based on first-order shear deformation plate theory (FSDPT). Sohn and Kim[5] dealt with the structural stability boundary of FG panels for temperature independent material characteristics. The influence of the aerodynamic loads and effect of asymmetric properties of the materials on flutter characteristics of the panel are examined in detail. The limit-cycle oscillation of a cantilever plate was studied by Weiliang and Dowell [6]. They employed a Rayleigh–Ritz approach in conjunction with the direct numerical integration and showed that the length-to-width ratio of the cantilever plate is a significant factor on the flutter study. Non-linear oscillations of a functionally graded FG plate are investigated by addadpour et al. [7] and simply supported [8,9] fluttering plates was studied using the Galerkin's method. Dowell [10,11] also investigated the nonlinear flutter of doubly curved panels of shallow curvature by using a modified form of the Donnell's nonlinear shallow-shell theory. He showed that stream-wise curvature is dramatically destabilizing for the onset of flutter.

In this paper, dynamic stability boundary for an FG panel in supersonic airflow is investigated using finite element method. The first-order shear deformation plate theory (FSDPT) is used and governing equations are derived from the principle of virtual work. Panel flutter boundaries are defined by eigen analysis. Guyan reduction is used to reduce the number of degree of freedom of the eigen-value problems. Temperature dependent material properties are assumed to take consideration for the high temperature environments. Effects of the tem- perature on material properties, Rayleigh damping

Sang-Lae Lee is with the School of Mechanical and Aerospace Engineering, Seoul National University, San 56-1, Sillim-Dong, Gwanak-Gu, Seoul 151-742, Korea (e-mail : winter10@snu.ac.kr).

Ji-Hwan Kim is with the School of Mechanical and Aerospace Engineering, Seoul National University, San 56-1, Sillim-Dong, Gwanak-Gu, Seoul 151-742, Korea (corresponding author to provide phone: +82-2-880-7383; fax: +82-2-887-2662; e-mail : jwhkim@snu.ac.kr).

coefficient, power law index and geometrical boundary on stability boundary of FG panel are studied in detail.

## II. MODELING OF FG PANELS

Fig. 1 shows a coordinate system and geometry of a ceramic-metal FG panel model with a length 'a', width 'b' and thickness 'h' which is subjected to supersonic airflow and thermal loads. A simple power law distribution is adopted, thus the volume fractions of the ceramic and metal are expressed:

$$V_c(z) = \left(\frac{z}{h}+\frac{1}{2}\right)^k (0 \le k < \infty), \quad V_m = 1 - V_c \quad (1)$$

where, $V$, the superscript $k$, the subscripts $c$ and $m$ denote the volume fraction, the volume fraction index, ceramic and metal, respectively. The material properties of FG panel can be obtained by a linear rule of mixture as follows:

$$P_{\text{eff}}(T,z) = P_m(T)V_m(z) + P_c(T)V_c(z) = P_c(T) + (P_m(T) - P_c(T))\left(1 - \frac{z}{h}\right)^k \quad (2)$$

where, $P_{\text{eff}}, P_m$ and $P_c$ are the effective material property, the material properties of the metal and ceramic, respectively.

Material properties of constituents must be dependent on temperature, since FGMs can be used in high temperature environments. The properties, $P$, of the ceramics and metals used as a mixture of FGMs can be expressed as [3] ;

$$P(T) = P_0\left(\frac{P_{-1}}{T} + 1 + P_1 T + P_2 T^2 + P_3 T^3\right) \quad (3)$$

in which P0, P-1, P1, P2 and P3 are the effective material properties and the coefficients of temperature.

Using the (1)–(3), the modulus of elasticity $E$, the coefficient of thermal expansion $\alpha$, the density $\rho$ and the thermal conductivity $K$ are written as:

$$E(T,z) = (E_c(T) - E_m(T))\left(\frac{z}{h}+\frac{1}{2}\right)^k + E_m(T)$$

$$\alpha(T,z) = (\alpha_c(T) - \alpha_m(T))\left(\frac{z}{h}+\frac{1}{2}\right)^k + \alpha_m(T)$$

$$\quad (4)$$

$$\rho(T,z) = (\rho_c(T) - \rho_m(T))\left(\frac{z}{h}+\frac{1}{2}\right)^k + \rho_m(T)$$

$$K(z) = (K_c - K_m)\left(\frac{z}{h}+\frac{1}{2}\right)^k + K_m$$

Here the thermal conductivity $K$ are assumed to be independent of temperature and the Posson's ratio $v$ is assumed to be constant as 0.3.

### A. Constitutive Equations

Based on the first-order shear deformation theory of plate, the displacement fields for the panel can be expressed as:

$$u(x,y,z,t) = u_0(x,y,t) + z\phi_x(x,y,t)$$

$$v(x,y,z,t) = v_0(x,y,t) + z\phi_y(x,y,t) \quad (5)$$

$$w(x,y,z,t) = w_0(x,y,t)$$

where $u$, $v$ and $w$ are the displacements in the $x$, $y$, and $z$ directions and $\phi_x, \phi_y$ are the rotations of the normal in the $xz$ and $yz$ planes, respectively, while the subscript '0' denotes the mid-plane.

Using the von-Karman strain-displacement relations, the strain vectors are expressed as:

$$\{e\} = \{\varepsilon\} + z\{\kappa\}$$

$$\{\gamma\} = \{\gamma_{yz} \quad \gamma_{xz}\}^T \quad (6)$$

where, $\{\varepsilon\}$ and $\{\kappa\}$ are the in-plane strain, the curvature strain at the mid-plane, respectively. Additionally, $\{\varepsilon\}, \{\kappa\}$ and $\{\gamma\}$ are given as:

$$\{\varepsilon\} = \{u_{,x} + \frac{1}{2}w_{,x}^2 , v_{,y} + \frac{1}{2}w_{,y}^2 , u_{,y} + v_{,x} + w_{,y}w_{,x}\}^T$$

$$\{\kappa\} = \{\phi_{x,x} , \phi_{y,y} , \phi_{x,y} + \phi_{y,x}\}^T \quad (7)$$

$$\{\gamma\} = \{w_{,y} + \phi_y , w_{,x} + \phi_x\}^T$$

The constitutive equations for the panels can be written as,

$$\begin{Bmatrix} \mathbf{N} \\ \mathbf{M} \end{Bmatrix} = \begin{bmatrix} \mathbf{A} & \mathbf{B} \\ \mathbf{B} & \mathbf{D} \end{bmatrix} \begin{Bmatrix} \boldsymbol{\varepsilon} \\ \boldsymbol{\kappa} \end{Bmatrix} - \begin{Bmatrix} \mathbf{N_{\Delta T}} \\ \mathbf{M_{\Delta T}} \end{Bmatrix}, \quad \mathbf{Q} = \mathbf{S}\boldsymbol{\gamma} \quad (8)$$

where, $\mathbf{N_b}$, $\mathbf{M_b}$ and $\mathbf{Q}$ denote the in-plane force resultant, the moment resultant and the transverse shear force resultant vectors, respectively. Meanwhile, $\mathbf{N_{\Delta T}}$ and $\mathbf{M_{\Delta T}}$ are the thermal in-plane force resultant and the thermal moment resultant vectors, which are given as:

$$(\mathbf{N_{\Delta T}}, \mathbf{M_{\Delta T}}) = \{N_{\Delta Tx}, N_{\Delta Ty}, N_{\Delta Txy}\}^T$$

$$= \int_{-h/2}^{h/2} (1,z)\mathbf{E}\{\alpha(z), \alpha(z), 0\}^T \Delta T(z) \, dz \quad (9)$$

The temperature elevation is defined as $\Delta T(z) = T(z) - T_0$ where $T_0$ is the reference temperature and $T(z)$ is the temperature distribution through the thickness.

The elastic coefficient matrix is:

$$\mathbf{E} = \frac{E(z)}{1-v^2} \begin{bmatrix} 1 & v & 0 \\ v & 1 & 0 \\ 0 & 0 & \frac{1-v}{2} \end{bmatrix}$$

while, $\mathbf{A}, \mathbf{B}, \mathbf{D}$ and $\mathbf{S}$ are the in-plane, the in-plane-bending coupling stiffness, the bending stiffness and the transverse shear stiffness matrices, which are given as:

$$(\mathbf{A}, \mathbf{B}, \mathbf{D}) = \int_{-h/2}^{h/2} \mathbf{E}(1, z, z^2) dz \quad (10)$$

$$\mathbf{S} = \kappa_p \int_{-h/2}^{h/2} \frac{E(z)}{2(1+v)} \begin{bmatrix} 1 & 0 \\ 0 & 1 \end{bmatrix} dz \quad (11)$$

where, $E(z)$ is the elastic modulus of an FG panel and the shear correction factor, $\kappa_p$, is assumed as $5/6$.

The temperature variation is assumed to occur in the thickness direction only and the temperature field is considered

constant in the $xy$ plane. In this case, the temperature through thickness is governed by the one-dimensional Fourier equation of heat conduction:

$$\frac{d}{dz}\left[K(z)\frac{dT}{dz}\right]=0 \;,\quad \begin{array}{l} T=T_c \text{ at } z=h/2 \\ T=T_m \text{ at } z=-h/2 \end{array} \tag{12}$$

where, $T_m$ and $T_c$ are temperature of the metal and ceramic, respectively.

Using the solution in [3], temperature distribution across the plate thickness becomes:

$$T(z)=T_m+(T_c-T_m)\Gamma(z) \tag{13}$$

where,

$$\Gamma(z)=\frac{1}{C}\left[\begin{array}{l}\left(\frac{2z+h}{2h}\right)-\frac{K_{cm}}{(k+1)K_m}\left(\frac{2z+h}{2h}\right)^{k+1}+\frac{K_{cm}^2}{(2k+1)K_m^2}\left(\frac{2z+h}{2h}\right)^{2k+1} \\ -\frac{K_{cm}^3}{(3k+1)K_m^3}\left(\frac{2z+h}{2h}\right)^{3k+1}+\frac{K_{cm}^4}{(4k+1)K_m^4}\left(\frac{2z+h}{2h}\right)^{4k+1}-\frac{K_{cm}^5}{(5k+1)K_m^5}\left(\frac{2z+h}{2h}\right)^{5k+1}\end{array}\right]$$

for,

$$C=1-\frac{K_{cm}}{(k+1)K_m}+\frac{K_{cm}^2}{(2k+1)K_m^2}-\frac{K_{cm}^3}{(3k+1)K_m^3}+\frac{K_{cm}^4}{(4k+1)K_m^4}-\frac{K_{cm}^5}{(5k+1)K_m^5}$$

and $K_{cm}=K_c-K_m$.

### B. Governing Equations

The governing equations for FG panel is obtained by using the principle of virtual work as follows

$$\delta W = \delta W_{\text{int}} - \delta W_{\text{ext}} = 0 \tag{14}$$

where $\delta W_{\text{int}}$ and $\delta W_{\text{ext}}$ represent internal and external virtual work, respectively, which are given as,

$$\delta W_{\text{int}} = \int_V \delta \mathbf{e}^{\mathbf{T}}\boldsymbol{\sigma}dV$$

$$=\int_A\left[\delta\boldsymbol{\varepsilon}^{\mathbf{0T}}\mathbf{N_b}+\delta\boldsymbol{\kappa}^{\mathbf{T}}\mathbf{M_b}+\delta\boldsymbol{\gamma}^{\mathbf{T}}\mathbf{Q}\right]dA \tag{15}$$

$$=\delta\mathbf{d^T}\left[\mathbf{K}-\mathbf{K_{\Delta T}}+\frac{1}{2}\mathbf{N1}+\frac{1}{3}\mathbf{N2}\right]\mathbf{d}-\delta\mathbf{d^T}\mathbf{P_{\Delta T}}$$

$$\delta W_{\text{ext}} = \int_A\Big[-I_0\left(\ddot{u}_0\delta u_0+\ddot{v}_0\delta v_0+\ddot{w}_0\delta w_0\right)$$

$$-I_1\left(\ddot{u}_0\delta\phi_x+\ddot{\phi}_x\delta u_0+\ddot{v}_0\delta\phi_y+\ddot{\phi}_y\delta v_0\right)$$

$$-I_2(\ddot{\phi}_x\delta\phi_x+\ddot{\phi}_y\delta\phi_y)+p_a\delta w\Big]dA \tag{16}$$

$$=-\delta\mathbf{d^T}\mathbf{M}\ddot{\mathbf{d}}+\delta\mathbf{d^T}\mathbf{f}$$

where, $\mathbf{d}=[\mathbf{u,v,w,\phi_x,\phi_y}]^T$ is the displacement vector and $(I_0,I_1,I_2)=\int_{-h/2}^{h/2}\rho(z)\cdot(1,z,z^2)dz$. In addition, $\mathbf{P_{\Delta T}}$, $\mathbf{K}$, $\mathbf{K_{\Delta T}}$, $\mathbf{N1}$, $\mathbf{N2}$, $p_a$, $\mathbf{M}$ and $\mathbf{f}$ are the thermal load vector, the linear elastic stiffness, the thermal geometric stiffness, the first-order nonlinear stiffness, the second-order nonlinear stiffness matrices, the aerodynamic pressure the mass matrix and the external force induced by thermal load, respectively.

The aerodynamic pressure is expressed by using the quasi-steady first-order piston theory [12],

$$p_a(x,y,t)=-\frac{\rho_a V_\infty^2}{\sqrt{M_\infty^2-1}}\left(\frac{\partial w}{\partial x}+\frac{1}{V_\infty}\frac{M_\infty-2}{M_\infty-1}\frac{\partial w}{\partial x}\right)$$

$$=-\left(\lambda\frac{D}{a^3}\frac{\partial w}{\partial x}+g_a\frac{\partial w}{\partial t}\right) \tag{17}$$

where

$$\lambda=\frac{\rho_a V_\infty^2 a^3}{\beta D}\;,\; D=\frac{E_m h^3}{12(1-\nu^2)}\;,\; g_a=\frac{\rho_a V_\infty(\beta^2-1)}{\beta^3\rho h\omega_0}\;,\; \beta=\sqrt{M_\infty^2-1}\;,\; \omega_0=\left(\frac{D}{\rho_a h a^4}\right)^{\frac{1}{2}}$$

in here $\rho_a, V_\infty, M_\infty, \beta, D, \omega_0, g_a, \lambda$ and $a$ represent the air mass density, the velocity of airflow, the Mach number, the aerodynamic pressure parameter, the flexural stiffness matrix, the convenient reference frequency, the non-dimensional aerodynamic damping, non-dimensional aerodynamic pressure and the panel length, respectively.

Using (17), the last term of (15) can be written in the form as:

$$\delta\mathbf{d^T}\mathbf{f}=\int_A p_a\delta w\, dA$$

$$=-\int_A\left(\lambda\frac{D}{a^3}\frac{\partial w}{\partial x}+\frac{g_a}{\omega_0}\frac{D}{a^4}\frac{\partial w}{\partial t}\right)\delta w\, dA=-\delta\mathbf{d^T}\left(\lambda\mathbf{A_f}\mathbf{d}+\frac{g_a}{\omega_0}\mathbf{A_d}\dot{d}\right) \tag{18}$$

where, $\mathbf{A_f}$, $\mathbf{A_d}$ denote the aerodynamic pressure matrix and the aerodynamic damping matrix, respectively.

Substituting (18) into (16) and then reinsert (16) and (15) into (14) gives the discretized form of governing equations obtained as:

$$\mathbf{M}\ddot{\mathbf{d}}+\mathbf{C}\dot{\mathbf{d}}+\left(\mathbf{K}-\mathbf{K_{\Delta T}}+\lambda\mathbf{A_f}+\frac{1}{2}\mathbf{N1}+\frac{1}{3}\mathbf{N2}\right)\mathbf{d}=\mathbf{P_{\Delta T}} \tag{19}$$

where, $\mathbf{C}=(\alpha\mathbf{M}+\beta\mathbf{K})+\dfrac{g_a}{\omega_0}\mathbf{A_d}$. In here, $\alpha$ and $\beta$ is the Rayleigh damping coefficients, where they are mass and stiffness proportional damping constants, respectively. The equation "$(\alpha\mathbf{M}+\beta\mathbf{K})$" denotes structural damping.

The solution of (19) is assumed as $\mathbf{d}=\mathbf{d_s}+\Delta\mathbf{d_t}$, where $\mathbf{d_s}$ and $\mathbf{d_t}$ represent the time independent and time dependent solutions, respectively. Substituting the assumed solution into (19), we can obtain two sets of coupled governing equations as follows.

$$\left(\mathbf{K}-\mathbf{K_{\Delta T}}+\lambda\mathbf{A_f}+\frac{1}{2}\mathbf{N1_s}+\frac{1}{3}\mathbf{N2_s}\right)\mathbf{d_s}=\mathbf{P_{\Delta T}} \tag{20}$$

$$\mathbf{M}\ddot{\mathbf{d}}_t+\mathbf{C}\dot{\mathbf{d}}_t+\left(\mathbf{K}-\mathbf{K_{\Delta T}}+\lambda\mathbf{A_f}+\frac{1}{2}\mathbf{N1_t}+\frac{1}{3}\mathbf{N2_t}+\mathbf{N2_{st}}+\frac{1}{2}\mathbf{N1_s}+\frac{1}{3}\mathbf{N2_s}\right)\mathbf{d_t}=0 \tag{21}$$

where, the subscript $s$ and $t$ represent the static and dynamic state, respectively.

The (20) is used for the static problem, post-buckling analysis, and the (21) is for the dynamic problem such as flutter boundary and flutter. A small incremental time dependent solution, $\Delta\mathbf{d_t}$, is assumed and to linearize (21) the time dependent nonlinear stiffness matrices, $\mathbf{N1_t}$, $\mathbf{N2_t}$ and $\mathbf{N2_{st}}$, become zero. Then the incremental equilibrium equation is expressed as:

$$\mathbf{M}\Delta\ddot{\mathbf{d}}_t + \mathbf{C}\Delta\dot{\mathbf{d}}_t + \left(\mathbf{K} - \mathbf{K}_{\Delta T} + \lambda\mathbf{A}_r + \mathbf{N1}_s + \mathbf{N2}_s\right)\Delta\mathbf{d}_t = \mathbf{0} \qquad (22)$$

A small amplitude vibration is assumed as $\Delta\mathbf{d}_t = \boldsymbol{\varphi}_0 e^{\omega t}$ and degree of freedom is reduced by Guyan reduction. Then, the reduced homogeneous equations for eigen analysis with state variables are written as

$$\left[ \begin{bmatrix} \mathbf{0} & \mathbf{M_R} \\ \mathbf{K_R} & \mathbf{C_R} \end{bmatrix} - \omega \begin{bmatrix} \mathbf{M_R} & \mathbf{0} \\ \mathbf{0} & -\mathbf{M_R} \end{bmatrix} \right] \begin{Bmatrix} \varphi_0 \\ \dot{\varphi}_0 \end{Bmatrix} = 0 \qquad (23)$$

where, $\mathbf{M_R}, \mathbf{K_R}$ and $\mathbf{C_R}$ are reduced mass, stiffness, damping matrices, respectively.

As $\lambda$ increases gradually from zero, two of these eigen-values will approach each other and coalesce to $\omega^*{}_{cr}$ at $\lambda = \lambda_{cr}$. After that they become complex conjugate pairs such that $\omega = \omega_r \pm i\omega_i$ for $\lambda > \lambda_{cr}$. From here, the panel flutter occurs. The non-dimensional frequency, $\omega^*{}_{cr}$, in the figure is defined as:

$$\omega^* = \left| \omega a^2 \sqrt{\frac{\rho_m h}{D_m}} \right| \qquad (24)$$

### III. NUMERICAL RESULTS AND DISCUSSIONS

Various kinds of materials are used as a mixture of FGMs such as $Al_2O_3 / Ni$, $SUS304/Si_3N_4$, Aluminum Oxide/Ti-6Al-4V and $SiC/Al$. Among these, we select a mixture of material such as $SUS304/Si_3N_4$, and then will investigate the flutter boundary of the panels in supersonic airflows. Also the model is made up of temperature dependent materials with a square shape. In the finite element modeling, a $6 \times 6$ mesh is used, and nine-node plate element is chosen. Additionally, a selectively reduced integration (SRI) technique [13] is employed to prevent the transverse shear locking phenomena for thin plate model using first-order shear deformation theory. For the nonlinear analysis, the Newton-Raphson iteration scheme is adopted to obtain approximate solutions and flutter boundary of FG panel subjected to supersonic aerodynamic loads are to be presented for two types of temperature variation such as uniform and gradient changes.

#### A. Code Verifications

First, the thermal post-buckling behaviors of simply supported FG panel for $k = 1$ are compared with previous data as shown in Fig. 2. In the diagram, "A" denotes the curves for temperature dependent material properties. While, the group "B" represents the results for temperature independent material properties calculated just only at reference temperature, 300K. In here, the results of the groups "A" and "B" show good agreements for each case. Next, the critical pressures of simply supported FG panels for various volume fractions are compared with [3]. The results are shown in Table III and agree well with that of previous work.

#### B. Stability Boundary of FG Panels

The stability boundary of panel under the combined aerodynamic and thermal loads is studied. FG panels are composed of Silicon-Nitride ($Si_3N_4$) and stainless steal ($SUS304$), and investigated in this study. Material properties are assumed to be dependent on the temperature and given in [14]. The reference temperature is taken as $T_0 = 300K$.

The critical aerodynamic pressure point is shown in Fig. 3. As non-dimensional aerodynamic pressure, $\lambda$, are monotonously increased from zero and then two eigen-values merges. Here, $\lambda_{cr}$ is considered to be the value $\lambda$ at which the first coalescence occurs.

In flutter boundary figure, there are four types of panel behavior: flat and stable, aero-thermally buckled but dynamically stable, flutter (limit cycle oscillation) and chaos. Generally, thermal stresses can lower the flutter boundary of panels. With increasing of the temperature of panels, the critical dynamic pressure decreases.

The critical fluttering value of various FG panels subject to thermal and aerodynamic loads with gradient temperature change are listed in Table III. This comparison of the data reveals that the critical aerodynamic pressures of the temperature dependent material case [3] is lower than that of the temperature independent material case [5] as shown. The reason may be originated from that internal thermal load leads the more thermally induced panels to flutter at lower temperature than temperature independent material.

Table IV presents critical fluttering value and frequencies of all simply supported and structural damped FG panels without thermal effect such as $T_m = T_c = 300K$. It is recognized that structural damping don't influence the critical value, however, enhances a decrease of the limit cycle frequency. This is due to the effect of structural damping which induces structure more flexible. Because of this, the limit cycle frequency of structural damped FG panels is decreased comparing the undamped ones.

Fig. 4 depicts stability boundaries of all clamped square FG panels with uniform temperature changes. At the region 'A' in the figure, the panels are flat and both statically and dynamically stable. In the region 'B', the panels are buckled but dynamically stable. The region 'C' represents dynamically unstable region where flutter occurs. In this region, a panel oscillates from its static equilibrium position with a self-exited harmonic motion. The region 'D' is a chaotic region in which chaotic motion happens in this region. [8] From the figure, it is noted that both the critical aerodynamic pressures for panel flutter and the critical temperature for thermal buckling increase, as the volume fraction index decreases. Flutter boundaries of all simply supported square FG panels is shown in Fig. 5. It is similar characteristics to the clamped cases. However, the critical aerodynamic pressure for flutter is lower than clamped one.

### IV. CONCLUSION

Functionally Graded (FG) panels are investigated for flutter boundary under thermal and aerodynamic loads. First-order shear deformation theory (FSDT) of the plate is applied to

model the panel, and the von-Karman strain-displacement relations are adopted to account for large deflection. Further, the first-order piston theory is used to model the supersonic aerodynamic load. Material properties are assumed as temperature-dependent, and this is one of the essential features of the material at high temperature environments. Main aim of this study is to estimate the effect of temperature dependent characteristics of flutter boundary of the FG panel composed of SUS304/Si$_3$N$_4$, and the results are discussed. It is concluded that the critical aerodynamic pressure decrease, as the value of volume fraction index, $k$, increases and the critical flutter velocity of a homogenous ceramic panel is the maximum among those of all panels. Comparing with isotropic metal panel ( Si$_3$N$_4$ ), FG panels have a merit for flutter characteristics. For more understanding the characteristics deviation due to the temperature and aerodynamic effects on the FG panels for applications, more parameter studies are required such as various mixture of materials, high temperature conditions and so on.

REFERENCES

[1] S. Suresh and A. Mortensen, "Fundamentals of functionally graded materials" *IOM Communications Ltd.* pp.3-7, 1998
[2] Noda N. "Thermal residual stresses in functionally graded materials". *J Therm Stress.*, vol.22, pp.477–512,1999
[3] T.Prakash and M.Ganapathi, "Supersonic flutter characteristics of functionally graded flat panels including thermal effects", *Composite Structures.,* vol. 72, no. 1, pp.10-18, 2006,
[4] G. N. Praveen and J. N. Reddy, "Nonlinear transient thermoelastic analysis of functionally graded ceramic–metal plates". *Int J Solids Struct.,* vol. 35, no. 33, pp.4457–4476, 1998,
[5] K. J. Sohn and J. H. Kim, "Structural stability of functionally graded panels subjected to aero-thermal loads", *Composite Structures.,* to be publication, 2007,
[6] Y. E. Weiliang and H. Dowell, "Limit cycle oscillation of a fluttering cantilever plate", *AIAA J.,* vol. 29, no. 11, pp.1929–1936, 1991,
[7] H. Haddadpour, H. M. Navazi and F. Shaadmehri, "Nonlinear oscillations of a fluttering functionally graded plate", *Composite Structures,* vol. 79, no. 2, pp. 242-250, 2007,
[8] E. H. Dowell, "Nonlinear oscillations of a fluttering plate". *AIAA J.,* vol. 4, no. 7, pp.1267–1275, 1966,
[9] E. H. Dowell, "Nonlinear oscillations of a fluttering plate II". *AIAA J.,* vol. 5, no. 10, pp.856–862, 1967,
[10] E. H. Dowell, "Nonlinear flutter of curved plates", *AIAA J.,* vol. 7, no. 3, pp.424–431, 1969,
[11] E. H. Dowell, "Nonlinear flutter of curved plates, II". *AIAA J.,* vol. 8, no. 2, pp. 259–261, 1970
[12] H. Ashley and G, Zartarian, "Piston Theory-A New Aerodynamic Tools for the Aeroelastician", *J Aeronautical Science.,* vol. 23, no. 12, pp.1109-1118, 1956,
[13] O. C. Zienkiewicz, R. L. Taylor, and J. M. Too, "Reduced integration technique in general analysis of plates and shells", *Int J Numerical Methods in Engineering,* vol. 3, pp.275-290, 1971,
[14] J. S. Park and J. H. Kim, "Thermal postbuckling and vibration analyses of functionally graded plates", *J Sound and Vibration,* vol. 289, pp.77-93, 2006

TABLE I
MATERIAL PROPERTIES OF FMGS FOR CERAMIC AND METAL [14]

| Materials | | $P_{-1}$ | $P_0$ | $P_1$ | $P_2$ | $P_3$ |
|---|---|---|---|---|---|---|
| $E$(Pa) | Si$_3$N$_4$ | 0 | 348.43 $\times 10^9$ | -3.070 $\times 10^{-4}$ | 2.160 $\times 10^{-7}$ | -8.946 $\times 10^{-11}$ |
| | SUS304 | 0 | 201.04 $\times 10^9$ | 3.070 $\times 10^{-4}$ | -6.534 $\times 10^{-7}$ | 0 |
| $\rho$ (Kg/m³) | Si$_3$N$_4$ | 0 | 2370 | 0 | 0 | 0 |
| | SUS304 | 0 | 8166 | 0 | 0 | 0 |
| $\alpha$ (1/K) | Si$_3$N$_4$ | 0 | 5.8723 $\times 10^{-6}$ | 9.095 $\times 10^{-4}$ | 0 | 0 |
| | SUS304 | 0 | 12.330 $\times 10^{-6}$ | 8.086 $\times 10^{-4}$ | 0 | 0 |

TABLE II
FLUTTER BOUNDARY OF TEMPERATURE DEPENDENT FGMS FOR UNIFORM
TEMPERATURE CHANGES (SI$_3$N$_4$/SUS304, $T_m = T_c = 300K$, A/H=20)

| Volume fraction ($k$) | Reference [3] | | Present | |
|---|---|---|---|---|
| | $\left\|\omega*_{cr}^2\right\|$ | $\lambda_{cr}$ | $\left\|\omega*_{cr}^2\right\|$ | $\lambda_{cr}$ |
| 0 | 9661.35 | 775.78 | 9663.2 | 776.1 |
| 0.5 | 4575.07 | 666.01 | 4575.3 | 669.1 |
| 1 | 3515.57 | 625.78 | 3515.6 | 624.2 |
| 2.5 | 2685.94 | 590.23 | 2689.8 | 592.3 |
| 5 | 2348.72 | 571.48 | 2348.6 | 574.1 |

TABLE III
FLUTTER BOUNDARY OF FG PANEL FOR GRADIENT TEMPERATURE CHANGES
(SI$_3$N$_4$/SUS304, $T_m = 300K$ and $T_c = 600K$, A/H=20)

| Volume fraction ($k$) | Reference [5] | Reference [3] | Present |
|---|---|---|---|
| | $\lambda_{cr}$ | $\lambda_{cr}$ | $\lambda_{cr}$ |
| 0 | 7950.8 | 7475.77 | 7468.2 |
| 0.5 | 3561.7 | 3381.36 | 3379.1 |
| 1 | 2683.5 | 2528.99 | 2520.9 |
| 2.5 | 1967.9 | 1849.33 | 1842.8 |
| 5 | 1684.9 | 1554.78 | 1548.3 |

TABLE IV
FLUTTER BOUNDARY OF FG PANEL DAMPED VERSUS UNDAMPED ONE
(SI$_3$N$_4$/SUS304, $T_m = T_c = 300K$, A/H = 20)

| Volume fraction ($k$) | Reference [5] (undamped) | | Present (damped) | |
|---|---|---|---|---|
| | $\left\|\omega*_{cr}^2\right\|$ | $\lambda_{cr}$ | $\left\|\omega*_{cr}^2\right\|$ | $\lambda_{cr}$ |
| 0 | 9660.1 | 771.8 | 9001.1 | 772.2 |
| 0.5 | 4573.6 | 663.0 | 3971.6 | 661.5 |
| 1 | 3513.2 | 623.1 | 2809.4 | 622.2 |
| 2.5 | 2698.2 | 588.0 | 2002.5 | 590.8 |
| 5 | 2350.7 | 568.7 | 1627.5 | 568.1 |
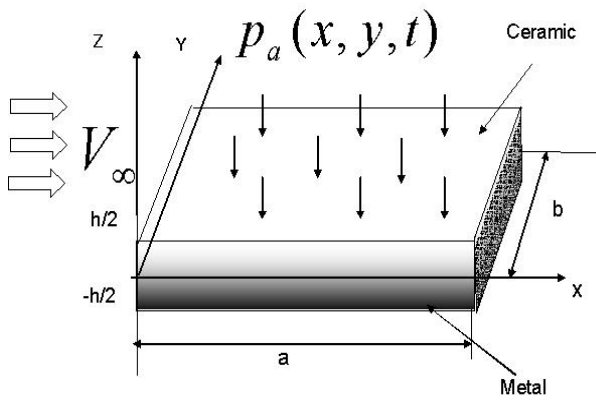
Fig. 1 Modeling of FG panel under supersonic airflow and thermal load



Fig. 4 Stability boundaries for various square panels
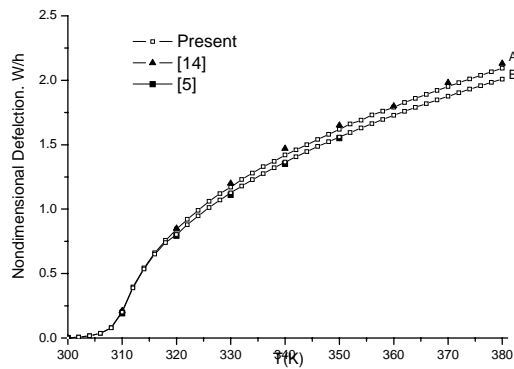(Clamped boundary condition, a/h=100)



Fig. 2 Thermal post-buckling behaviors of a square FG panel

(A: Temperature dependent, B: Temperature independent)



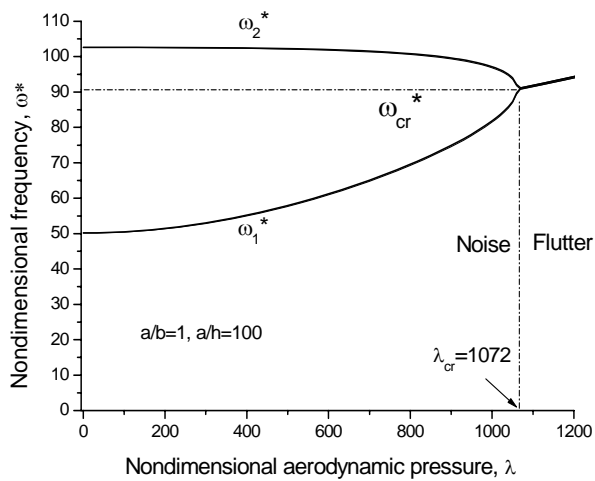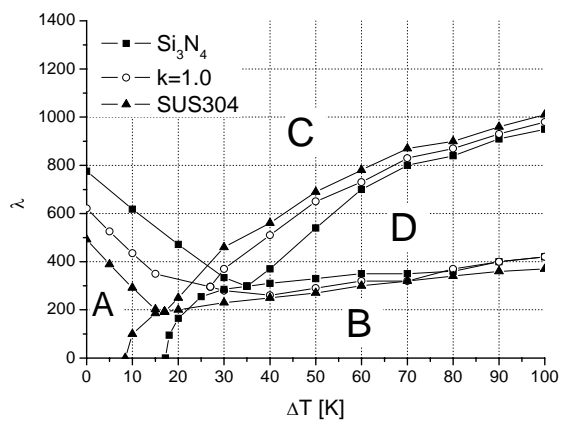Fig. 5 Stability boundaries for various square panels
(Simply supported boundary condition, a/h=100)



Fig. 3 Frequency coalescence for an FG panel ( $\Delta T = 0$, $k = 1.0$ )